

N 88-15633

532-27  
116734  
218

1987

NASA/ASEE SUMMER FACULTY RESEARCH FELLOWSHIP PROGRAM

MARSHALL SPACE FLIGHT CENTER  
THE UNIVERSITY OF ALABAMA IN HUNTSVILLE  
  
THE DEVELOPMENT OF TEST METHODOLOGY  
FOR TESTING GLASSY MATERIALS

Prepared By: Dennis S. Tucker  
Academic Rank: Assistant Professor  
NASA/MSFC:  
Laboratory: Materials and Processes  
Division: Non-Metallic Materials  
Branch: Ceramics and Coatings  
NASA Colleague: Ronald L. Nichols  
Contract No.: The University of Alabama  
in Huntsville 5-30109

## ABSTRACT

The inherent brittleness of glass invariably leads to a large variability in strength data and a time dependence in strength (i.e. static fatigue). Loading rate plays a large role in strength values. Glass is found to be weaker when supporting loads over long periods as compared to glass which undergoes rapid loading. In this instance the purpose of rapid loading is to fail the glass before any significant crack growth occurs. However, a decrease in strength occurs with a decrease in loading rate, pursuant to substantial crack extension. These properties complicate the structural design allowable for the utilization of glass components in applications such as mirrors for the Space Telescope and AXAF for Spacelab and the Space Station.

This report describes the test methodology to obtain strength and fracture mechanics parameters which can be used to predict the reliability and lifetimes of such glass components.

List of Figures

<u>Figure No.</u>	<u>Caption</u>
1	4-Point Bend Fixture
2	Double-Ring Bend Fixture
3	Typical Fracture Plot for a Brittle Material
4	Double Cantilever Beam Specimen Configuration
5	Edge Cracked, Three Point Bend Specimen for Determination of $K_{IC}$

### Nomenclature

a	Moment are in four-point bend test (Eq. 1)
b	Specimen width for four-point bend test (Eq. 1)
c <sub>o</sub>	Distance from neutral axis to outer fibers in a beam (Eq. 2)
C	Crack Length
d	Specimen thickness for four-point bend test (Eq. 1)
E	Young's Modulus
Δ F	Increase in test force (Eq. 3)
F <sub>max</sub>	Maximum force (Eq. 3)
I	Moment of inertia
K <sub>I</sub>	Stress intensity factory
K <sub>Ic</sub>	Critical stress intensity factor
L	Breaking load (Eq. 1)
ℓ	Crack length (Eq. 8)
m	Bending moment
r	Spatial distribution of stresses at a crack tip (Eq. 7)
s	Specimen thickness (Eq. 3 and 4)
S	Bending Stress
Δ t	Variation in time (Eq. 3)
Y	Dimensionless parameter (Eq. 8)
γ	Surface energy
f(θ)	Angular distribution of normal stresses at a crack tip
ν	Poisson's ratio
σ	Applied stress (Eq. 6)

Nomenclature

$\sigma_N$	Normal stress at a crack tip
$\sigma_2$	Applied stress (Eq. 8)
$\sigma^*$	Griffith stress
$\Delta\sigma_b$	Change in bending stress (Eq. 3)
$\sigma_{bB}$	Bending strength

#### ACKNOWLEDGEMENT

The author wishes to acknowledge the NASA/ASEE Summer Faculty Fellowship Program along with Gerald Karr, the UAH Director.

To NASA counterpart Ronald L. Nichols of the Ceramics and Coatings Branch, Non-Metallic Materials Division, gratitude is offered.

Thanks to Bill Kennedy, without whose assistance this work would not have progressed as well as it did.

## INTRODUCTION

The aim of this program is to provide the necessary data to predict and improve the reliability and lifetime of glass components which will be utilized in the following program applications:

- o AXAF Mirrors
- o Space Telescope Mirrors
- o Spacelab Windows
- o Space Station Windows
- o Future Space Structures
- o Equipment with Optical Lenses
- o Large Deployable Structures

The establishment of this investigation will be accomplished in three phases. Phase I will include the determination of materials properties, surface treatments, and inspection techniques for maximum flaw size detection. Phase II will be the development of a reliable structural model and Phase III will be model verification by sub-assembly testing and evaluation.

Due to time constraints this study will concentrate solely on Phase I, consisting of four tasks. The tasks are as follows:

Task I - Review and compilation of current properties, inspection techniques, surface treatments, and test methodologies of glass.

Task II - The effects of surface treatment on glass strength.

Task III - Utilization of various inspection techniques such as microscopy, polarization, XRD, thermography, ultrasonics to determine maximum flaw size existing in the glass.

Task IV - Materials property generation.

- o Design and fabricate the required test fixtures and equipment.

- o Selection candidate glass materials and prepare test specimens.
- o Test specimens with specific surface/thermal procedure.
- o Inspect the specimens with the most promising flaw detection techniques. Test materials to determine "A" basis properties of stress model parameters from the defined stress model equation.
- o Analyze the "A" basis properties data for required inclusion into the stress model.

Initial strength and delayed fracture techniques are used to generate materials properties in Task IV. Four point bending and double ring bending will be used to characterize initial strength properties. Delayed fracture properties will be developed utilizing fracture mechanics theory by establishing stress intensity factors and critical stress intensity factors for each glass system.

#### Technical Discussion

##### Initial Strength

Modulus of Rupture (MOR) will be determined using four point bend flexure testing<sup>1</sup> as shown in Figure 1. For this test the modulus of rupture is given by:

$$S = \frac{3LA}{bd^2} \quad (1)$$

where:

L = breaking load

a = moment arm

b = specimen width

d = specimen thickness.

This relationship can be readily derived from the formula for maximum bending stress in a rectangular beam. This formula is stated as:<sup>2</sup>

$$S = \frac{mc_o}{I} \quad (2)$$

where:

$S$  = maximum bending stress

$m$  = bending moment at any section (equal to the applied load times the moment arm)

$c_o$  = distance from the neutral axis to the outer fibers on which the stress acts

$I$  = moment of inertia.

The double ring bending strength test method will also be used to determine initial strength.<sup>3</sup> Figure 2 is a graphical representation of this technique. In this case a disc shaped specimen is loaded between two concentric rings. For limited forces, a tensile stress field will be set up in the central region of the convexly bent specimen surface. Outside the load ring the radial and tangential stresses in the specimen decrease towards the edge, so that the possibility of fracture there is small. By increasing the force the tensile stress in the specimen center is increased at a constant rate until fracture occurs, with the expectation that the fracture is initiated in the region of the surface subjected to the maximum stress, underneath the load ring. Obviously, a major advantage of this technique is the elimination of edge effects.

To calculate the rate of increase of the bending stress in circular specimens the following is applicable:

$$\frac{\Delta \sigma_b}{\Delta t} = \frac{1.08}{s^2} \cdot \frac{\Delta F}{\Delta t} \quad (3)$$

where:

$\Delta F$  = Increase of test force, measured in the time interval  $\Delta t$  near the fracture initiation.

$s$  = Specimen thickness.

1.08 = Numerical constant related to the load ring and specimen ring diameters and Poisson's ratio.

The bending strength ( $\sigma_{bB}$ ) belonging to the maximum force ( $F_{max}$ ) from the above equation is:

$$\sigma_{bB} = 1.08 \frac{F_{max}}{s^2} \quad (4)$$

where

$\sigma_b$  = bending strength

$F_{max}$  = greatest force

$s$  = specimen thickness.

### Delayed Fracture

(Fracture Mechanics Parameters)

It is well established that the fracture strength of glass is excellent when loaded in compression. However, in tension, strengths are substantially lower than the theoretical strength calculated on the basis of interatomic bonding.<sup>4</sup> It is understood that this decrease in strength is due to the presence of flaws which act as stress raisers. In glass these flaws are usually surface cracks. Griffith<sup>5</sup> developed a failure criterion based on an energy inventory at the crack tip; i.e., a crack will propagate in a material provided

$$\frac{\partial E}{\partial C} = \left[ \pi \sigma^2 C^2 \frac{1 - \nu^2}{E} + 4C\gamma \right] \leq 0 \quad (5)$$

where:

$C$  = crack length

$\sigma$  = applied stress

$E$  = Young's modulus

$\nu$  = Poisson's Ratio

$\gamma$  = Energy per unit area of surface created by fracture propagation.

When equation (5) is solved for  $\sigma$ , one obtains the Griffith stress:

$$\left( \frac{2\gamma E}{\pi C (1 - \nu^2)} \right)^{1/2} \equiv \sigma^* \quad (6)$$

Thus if the applied stress equals or exceeds the Griffith stress,  $\sigma^*$  the crack will propagate.

Although glass is relatively inert to most corrosive atmospheres, it is susceptible to stress corrosion caused by water in the environment. This phenomenon is known as stress corrosion, static fatigue, or delayed failure. Griffith failed to take this property into consideration in the determination of  $\sigma^*$  in equation 6, above. It is now believed that static fatigue results from the growth of small surface cracks until the crack length C, in equation 6, causes the stress to exceed  $\sigma^*$ . At this point catastrophic failure will occur.

One method for studying stress corrosion is to measure the velocity of macroscopic cracks as a function of selected variables such as load and environment. These experimental determinations are generally called fracture mechanics studies. Fracture mechanics is important in characterizing subcritical crack growth because the crack tip stresses that cause crack growth are directly proportional to the stress intensity factor.

The angular ( $\theta$ ) and spatial ( $r$ ) distribution of normal stresses at the tip of a crack,  $\sigma_N$ , for plane strain crack displacement can be given by:

$$\sigma_N = \frac{K_I f(\theta)}{(2\pi r)^{1/2}} \quad (7)$$

where  $K_I$  is the stress intensity factor. The subscript I stands for Mode I cracking (opening model). A simple dimensional analysis of a body containing a crack of length 2 subjected to an applied stress,  $\sigma_2$ , indicates that the stress enhancement at the crack is related to  $\sigma_2$  and  $\theta$  by:

$$K_I = \sigma_2 \sqrt{\ell} Y \quad (8)$$

Where  $Y$  is a dimensionless parameter depending upon the specimen and crack geometry.  $K$  is a measure for all stresses and strains. Crack extension will occur when the stresses and strains at the crack tip reach a critical value. This means that fracture is expected to occur when  $K_I$  reaches a critical value  $K_{Ic}$ . The critical value may be expected to be material parameter. A typical plot of stress intensity factor ( $K_I$ ) vs. Crack Growth and the definition of critical stress intensity factor ( $K_{Ic}$ ) is shown in Figure 3. Although the point called  $K_{Ic}$  is simply one point on the curve in Figure 3 it is useful for predicting critical flaw sizes or in calculations of impact or erosion behavior.

There are two generally accepted theories of delayed fracture. Charles and Hillig<sup>6</sup> stated that delayed fracture is due to a stress enhanced chemical reaction, with the parameters being stress intensity factor, environment of the crack tip (moisture content) and the character of the material itself. Wiederhorn's<sup>7</sup> stress corrosion studies have confirmed much of the Charles-Hillig theory. Hasselman<sup>8</sup> asserts that the micro-cracks grow by the stress enhanced, thermally activated formation of vacancies at the crack tip. This theory agrees well with data taken on a typical industrial glass.

The stress intensity factor is established for a brittle material utilizing a specimen with an initial crack of known length. The most common method of testing for  $K_I$  is the double cantilever beam technique as shown in figure 4. With this method a specimen is ground to force glass fracture in the central portion of the specimen. A crack is then initiated by localized thermal shock. The stress intensity factor is then determined by monitoring the crack growth relative to a controlled load. The advantage of this technique is that a constant moment rather than a constant load is applied<sup>9</sup>. This results in the strain energy release rate being independent of crack length. Also, corrections for shear or beam rotation are unnecessary.

Obviously this technique can be used to identify the critical stress intensity factor. Fracture toughness may also be obtained from three-point bend testing of a specimen with an initial edge crack (Figure 5).

#### Experimental Procedures

Completion of the materials testing was precluded by the short duration of the summer term.

Four optical grade glasses were selected for testing. These are: Corning's Ultra Low Expansion (ULE) titanium silicate glass, Schott's BK-7 glass and Zero-Dur glass and Corning's 7740 Pyrex glass. Twenty eight disc-shaped ULE glass specimens were coarse ground to a thickness of 6 mm. All were polished to a 400 grit finish. Half of these were then tested for MOR using the double ring bending method. The testing was performed using an Instron 1125 testing machine using a crosshead rate of 0.02 in/min. The remaining specimens will be further polished to a diamond finish and tested in the same manner.

It is planned to use either a one or two-stage replica technique to obtain information on flaw size and flaw size distribution. The technique basically consists of coating the sample surface with carb n or formvar and carbon. When the coating is removed it may then be examined by transmission electron microscopy. The disadvantage of this technique is that it only gathers details from the surface. Therefore, a means to investigate volume or bulk flaws is needed. A literature search is under way to elucidate if such a means exists.

#### RESULTS

Table I shows the results of the MOR test of the ULE glass samples. All samples were observed to fail centrally (i.e. under the load rings with cracks spreading radially to the specimen edge).

## CONCLUSIONS

1. Double ring bend fixture was machined to adapt to the Instron 1125 test machine.
2. A four-point bend fixture was ordered from the Instron Company.
3. Samples of ULE glass were polished to a 400 grit finish for testing by the double ring bend method.
4. Pyrex and BK-7 glasses were contracted to be cut and polished to produce specimens for four-point bend and double-ring bend tests.
5. Samples of Zero-Dur glass will be provided by Schott Glass Inc., for both MOR tests.

## Bibliography

1. "Flexure Testing of Glass", ASTM No. C158-72, 1984.
2. E. P. Popov, Introduction to Mechanics of Solids, Prentice-Hall, Inc., 1968.
3. "Testing of Glass and Glass Ceramics; Determination of Bending Strength", German Standard DK 666.151:620.174, April 1984.
4. E. Orowan, Inst. of Engineers and Shipbuilders in Scotland, 89, 165 (1945-6); Proc. of International Conference on Physics, The Physical Society, London, 2, 81, 1934.
5. A. A. Griffith, "The Phenomena of Rupture and Flow in Solids", Phil. Tran. Roy. Soc., (London), A221, 163 (1920-21).
6. R. J. Charles and W. B. Hillig, "The Kinetics of Glass Failure and Stress Corrosion", Symposium of Mechanical Strength and Ways of Improving It, Florence, Italy, 25-29, Sept. 1961, Union Scientifique Continentale du Verre, Charleroi, Belgium (1962), p. 511.
7. S. M. Wiederhorn, "Influence of Water Vapor on Crack Propagation in Soda-Lime Glass", J. Am. Cer. Soc., 50, 407 (1967).
8. D. P. H. Hasselman, "Proposed Theory for the Static Fatigue Behavior of Brittle Ceramics", Ultrafine-Grain Ceramics, Syracuse Univ. Press, Syracuse, N.Y. (1970), Chapt. 14.
9. S. W. Freiman, D. R. Mulville, and P. W. Past, "Crack Propagation Studies in Brittle Materials", J. of Mat. Sci., 8 (1973) pp. 1527-1533.

Figure 1.

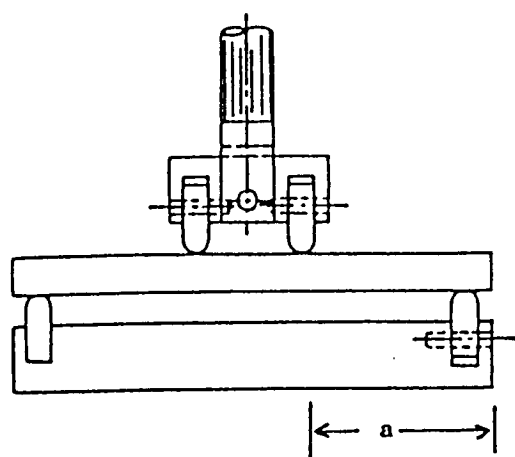


Figure 2.

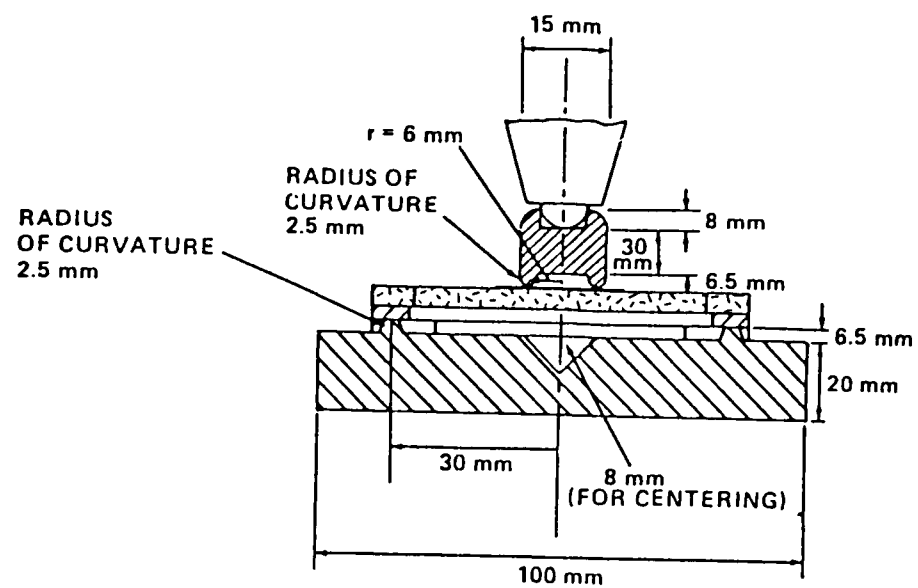


Figure 3.

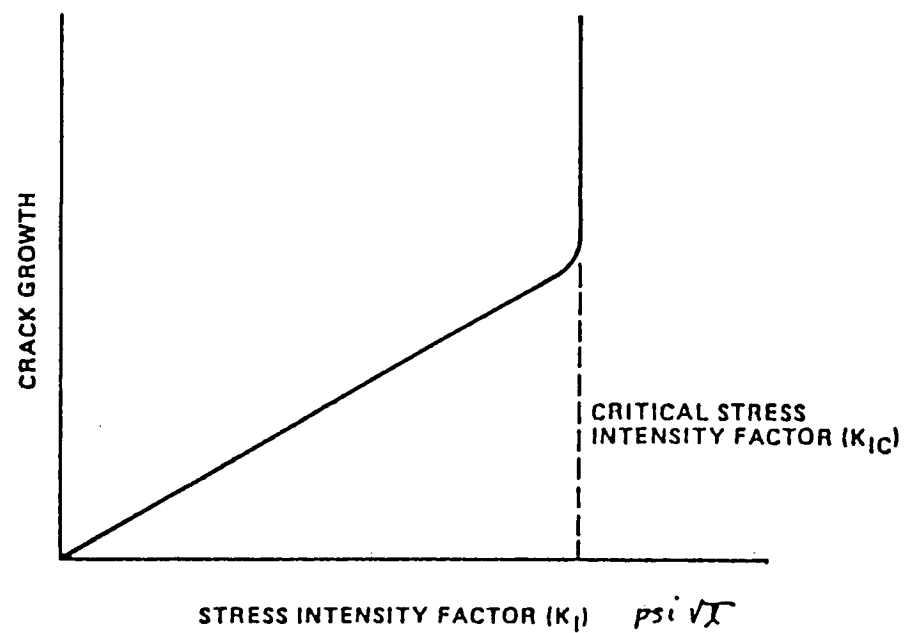


Figure 4.

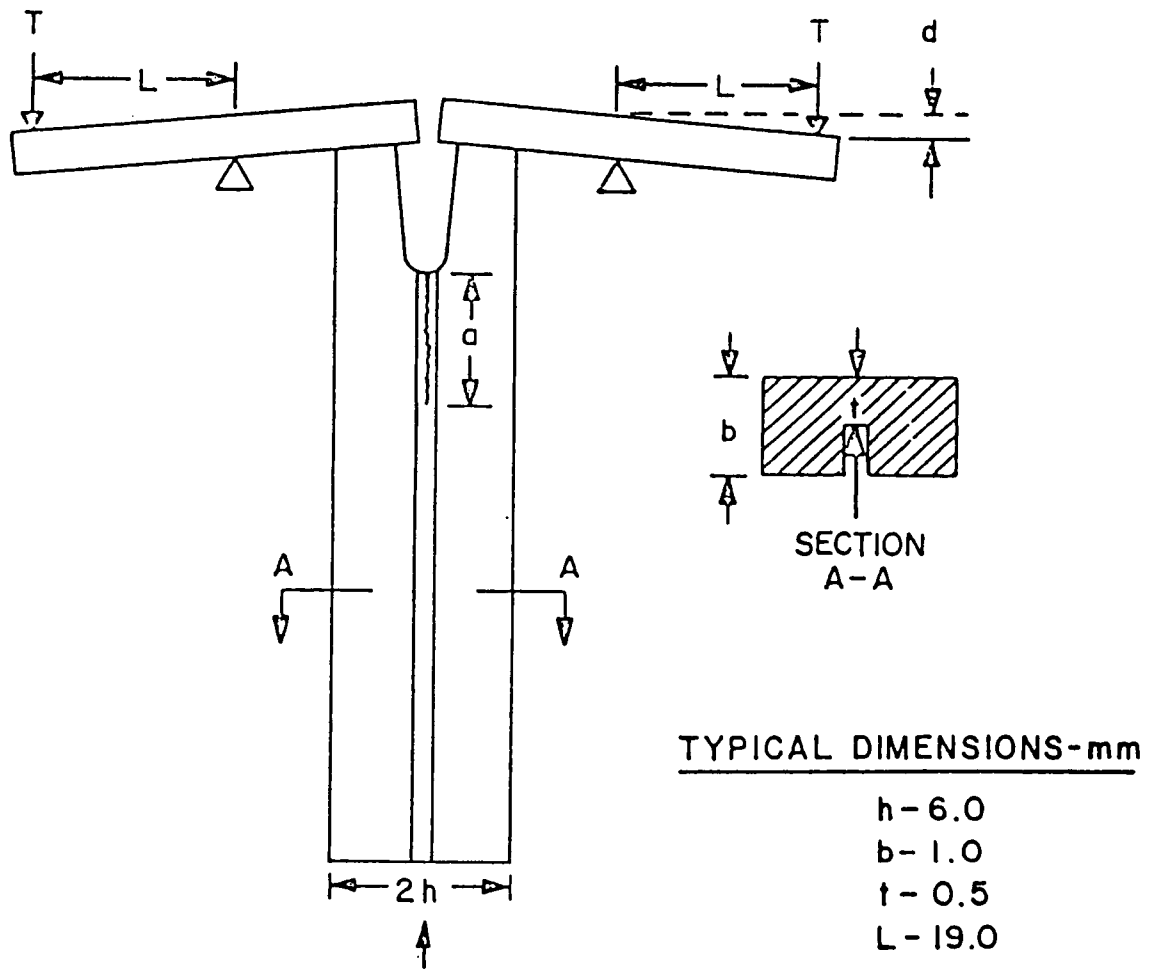


Figure 5.

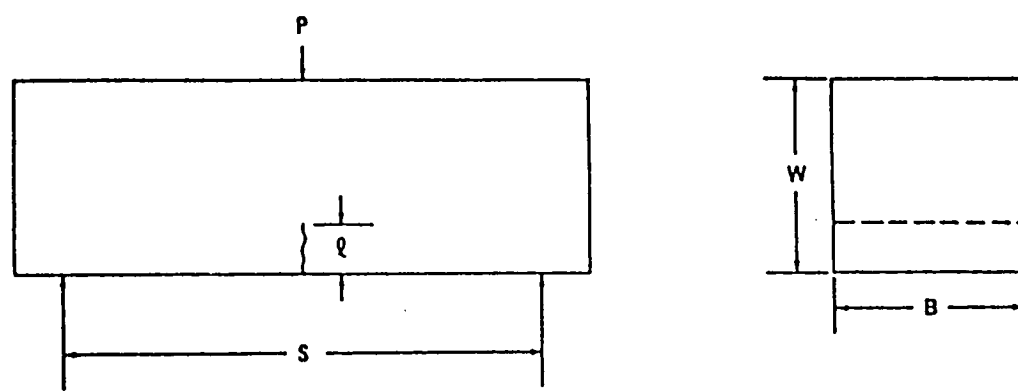


TABLE I - MOR OF ULE GLASS SAMPLES

<u>Sample No.</u>	<u>t (in.)</u>	<u>F max (lb)</u>	<u>MOR (psi)</u>
1	0.232	307	6140
2	0.231	235	4788
3	0.232	283	5660
4	0.231	302	6154
5	0.228	288	5981
6	0.233	400	8000
7	0.233	280	5600
8	0.230	440	8966
9	0.233	335	6700
10	0.234	230	4516